

Another close look at the spatial structure of CAR and SAR models

Renato Assunção^{a,*}, Elias Teixeira Krainski^a, Guido del Piño^b

^a*Universidade Federal de Minas Gerais, Departamento de Estatística, 31270-901
Belo Horizonte, MG, Brazil*

^b*Pontificia Universidad Católica, Facultad de Matemáticas, Campus San Joaquín,
Avenida Vicuña Mackenna 4860, Santiago, Chile*

Abstract

The conditional autoregressive model (CAR) and the simultaneous autoregressive model (SAR) are widely used to model the spatial correlation of lattice data. Several authors have pointed out impractical or counterintuitive consequences produced by these models for the covariance matrix. This paper clarifies many of these puzzling results. We show that the neighborhood graph structure, synthesized in eigenvalues and eigenvectors structure of a matrix associated with the adjacency matrix, determines most of the apparently anomalous behavior. We illustrate our conclusions with regular and irregular lattices including lines, grids and lattices based on real maps.

Key words: Spatial interaction, Lattice data, Spatial autoregression

1991 MSC: 62H11, 62E10

* Corresponding author.

Email addresses: `assuncao@est.ufmg.br` (Renato Assunção),

20 1 Introduction

21 Lattice data refer to statistical data observed at spatial locations or areas in a
22 given geographical region. It is common to assume that observations at sites
23 near each other tend to have similar values. The Conditional Autoregressive
24 (CAR) and the Simultaneous Autoregressive (SAR) models are widely used
25 to analyze these lattice data. The SAR model is preferred in likelihood infer-
26 ence, while the CAR model is more common in Bayesian inference as a prior
27 distribution for spatially structured random effects.

28 Despite their popularity, these models bring uneasy consequences for the im-
29 plied correlation structure of the variables. Several authors have pointed out
30 that the SAR and CAR models yield non constant variances at each site as
31 well as unequal covariances between regions separated by the same number of
32 neighbors (Haining, 1990, page 82; Besag and Kooperberg, 1995).

33 Wall (2004) extensively studied the covariance structure entailed by these
34 models. She found that the implied correlation between a pair of neighboring
35 areas is negatively associated with the number of neighbors of each region.
36 However, she also showed that this relationship is not simple and much vari-
37 ability remains unexplained. For example, considering the three neighboring
38 US states Missouri, Arkansas, and Tennessee, she showed that, although Mis-
39 souri and Tennessee have the same neighboring structure, their correlation
40 with Arkansas differs. She also showed that sites with equal number of neigh-
41 bors can have different variances.

ekrainski@ufmg.br (Elias Teixeira Krainski), gdelpino@mat.puc.cl (Guido del Piño).

42 In addition to these uncomfortable results, Wall (2004) pointed out a series of
 43 puzzling results from these two spatial models. One of them is that correla-
 44 tions between areas switch their ranks depending on ρ , a spatial dependence
 45 parameter. Suppose that a pair (i, j) of sites are more correlated than another
 46 pair (k, l) when $\rho = 0.5$. It is not uncommon that when $\rho = 0.7$, the pair (k, l)
 47 becomes more correlated than (i, j) . One would expect, perhaps naively, that
 48 the order should be the same, irrespective of the spatial dependence parame-
 49 ter value. Even more puzzling are the results concerning negative values for ρ .
 50 She found that when ρ is negative, correlations between the neighboring areas
 51 are also negative but, as ρ decreases further, some pairs of areas start to be
 52 positively correlated, even approaching +1 at times.

53 Wall (2004) concluded that the implied spatial correlation between the differ-
 54 ent sites using the SAR and CAR models does not seem to follow an intuitive
 55 or practical scheme and she called for more research to be carried out to clarify
 56 these problems. This is the main purpose of this paper. We explain the appar-
 57 ently counterintuitive or impractical consequences of the model specification
 58 by using the complete neighborhood graph structure, not only the immediate
 59 neighborhood. In accounting for the complete neighborhood structure, we see
 60 that a crucial role is played by the second largest eigenvalue modulus of the
 61 neighborhood matrix used in the SAR and CAR models. We use a simple
 62 matrix algebra identity to write the covariance matrices of the SAR and CAR
 63 models as a matrix power series. This enables us to express the correlation
 64 between any two pairs of areas i and j as an infinite series with exponential
 65 decay given by the spatial dependence parameter ρ . Moreover, the k -th term
 66 coefficient of this series is proportional to a weighted sum of the different paths
 67 to move from area i to area j in k steps.

68 In Section 2, the CAR and SAR models are defined and we illustrate the
 69 implied consequences for the covariance structure by means of an example
 70 with the US continental states. Section 3 reviews the linear algebra definitions
 71 and results relevant for this paper and Section 4 shows how many of the
 72 puzzling results can be understood. Conclusions are presented in Section 5.

73 2 The SAR and CAR models

74 Let a region D be partitioned into n areas $\{A_1, \dots, A_n\}$ such that $D = A_1 \cup$
 75 $\dots \cup A_n$ and $A_i \cap A_j = \emptyset$ for all $i \neq j$. Let y_i be a random variable measured at
 76 area i and $\mathbf{y} = (y_1, \dots, y_n)^t$. We denote by \mathbf{y}_{-i} the $(n-1)$ -dimensional vector
 77 without the i -th coordinate of \mathbf{y} . The conditional autoregressive model (CAR)
 78 is given by a set of n conditional distributions

$$79 \quad y_i | \mathbf{y}_{-i} \sim N \left(\mu_i + \sum_{j=1}^n c_{ij} (y_j - \mu_j), \kappa_i^2 \right) \quad (1)$$

80 where $c_{ii} = 0$ and $\kappa_i^2 > 0$ for $i = 1, \dots, n$. It is not any set of n conditional
 81 distributions that determine uniquely a joint distribution for the vector \mathbf{y} .
 82 However, a very popular choice in spatial studies for the constants c_{ij} and κ_i
 83 defines a valid joint model, and we adopt this choice in the rest of this paper.

84 The choice of the $n \times n$ matrix $\mathbf{C} = (c_{ij})$ is related to the degree of spatial
 85 proximity between areas i and j . Let $\mathbf{A} = (a_{ij})$ be an $n \times n$ binary neigh-
 86 borhood matrix such that $a_{ij} = 1$ if, and only if, areas i and j are neighbors
 87 (denoted by $i \sim j$). We let $a_{ii} = 0$. Define $\mathbf{W} = (w_{ij})$ such that $w_{ij} = a_{ij}/a_i$.
 88 where $a_i = \sum_j a_{ij} = d_i$, the number of neighboring areas of region i . Finally,
 89 define $\mathbf{C} = \rho_c \mathbf{W}$ and $\kappa_i = \sigma_c^2/d_i$. Under a restriction on the value of ρ_c , the

CAR model (1) with these options defines a valid joint distribution for the vector \mathbf{y} given by a multivariate normal distribution:

$$\mathbf{y} \sim N_n(\boldsymbol{\mu}, (\mathbf{I} - \rho_c \mathbf{W})^{-1} \mathbf{K}) \quad (2)$$

where $\boldsymbol{\mu} = (\mu_1, \dots, \mu_n)'$, \mathbf{I} is the identity matrix and \mathbf{K} is the diagonal matrix $\text{diag}(\kappa_1, \dots, \kappa_n)$ which is equal to $\sigma_c^2 \text{diag}(d_1^{-1}, \dots, d_n^{-1})$. The restriction on ρ_c is necessary to ensure that $(\mathbf{I} - \rho_c \mathbf{W})^{-1} \mathbf{K}$ is positive definite and it suffices to take ρ_c such that ρ_c is between $1/\min_i \lambda_i$ and $1/\max_i \lambda_i$ where $\lambda_i, i = 1, \dots, n$, are the eigenvalues of \mathbf{W} (Haining, 1990, page 82).

This choice also implies that (1) reduces to

$$y_i | \mathbf{y}_{-i} \sim N(\mu_i + \rho_c \overline{(y - \mu)_i}, \sigma_c^2 / d_i) \quad (3)$$

where $\overline{(y - \mu)_i} = \sum_j w_{ij}(y_j - \mu_j)$ is the average of the deviations $y_j - \mu_j$ among $j \sim i$, i.e. among the neighboring areas of i .

The SAR model is defined by n simultaneous equations

$$y_i = \mu_i + \sum_{j=1}^n s_{ij}(y_j - \mu_j) + \epsilon_i \quad (4)$$

where $\epsilon = (\epsilon_1, \dots, \epsilon_n)' \sim N(0, \mathbf{\Lambda})$ with $\mathbf{\Lambda}$ diagonal, $E(y_i) = \mu_i$, and s_{ij} are known constants with $s_{ii} = 0, i = 1, \dots, n$. This model is *simultaneous* because the random variables are simultaneously determined by the n equations in 4. Provided that the inverse of the matrix $I_n - S$ exists, the distribution of $\mathbf{y} = (y_1, \dots, y_n)'$ is

$$\mathbf{y} \sim N(\boldsymbol{\mu}, (I_n - S)^{-1} \mathbf{\Lambda} (I_n - S)^{-1'}) \quad (5)$$

where $S_{ij} = s_{ij}$. A popular choice for \mathbf{S} is to take $\mathbf{S} = \rho_s \mathbf{W}$, where $\rho_s \in (-1, 1)$. Following Wall (2004), we will constrain ρ_s to the same interval as ρ_c in order to allow for comparisons between the models.

With these choices for the SAR and CAR model, the correlation matrix entries are functions of only \mathbf{W} and ρ_c or ρ_s . For example, for the CAR model, we have

$$\text{Cor}(i, j) = \frac{\sigma_c^2 (I - \rho_c \mathbf{W})_{ij}^{-1} d_j^{-1}}{\sqrt{\sigma_c^2 (I - \rho_c \mathbf{W})_{ii}^{-1} d_i^{-1}} \sqrt{\sigma_c^2 (I - \rho_c \mathbf{W})_{jj}^{-1} d_j^{-1}}},$$

and σ_c^2 is canceled out.

2.1 The puzzling results

We summarize the main puzzling results concerning the correlations implied by the SAR and CAR models and described by Wall (2004). She used the United States map to illustrate the implications that the CAR and SAR models entail for the covariance between pairs of areas. Consider the graph composed by the 48 contiguous continental states. Two states i and j are connected by an edge (meaning that $w_{ij} > 0$) if they share borders. This graph is in Figure 1, with the underlying US map. The upper right plot in Figure 1 shows the correlations $\text{Cor}(i, j)$ between pairs of neighboring states by the number of neighbors. Every pair (i, j) of neighboring areas contribute two points in this plot depending on each area's number of neighbors, the pair $(d_i, \text{Cor}(i, j))$ and the pair $(d_j, \text{Cor}(i, j))$. We can see that, for a given number of neighbors, there is a large variation in the correlations.

The lower row of plots in Figure 1 shows how the correlations $\text{Cor}(i, j)$ varies

132 with the spatial dependence parameter ρ . Each line represents the correlation
 133 between two neighboring areas and the horizontal axis corresponds to the
 134 spatial dependence parameter ρ_s of the SAR model (left hand side plot), or
 135 ρ_c for the CAR model (right hand side plot). Based on the eigenvalues of \mathbf{W}
 136 for the US lattice, a restriction for the spatial parameter space $(-1.392, 1)$.

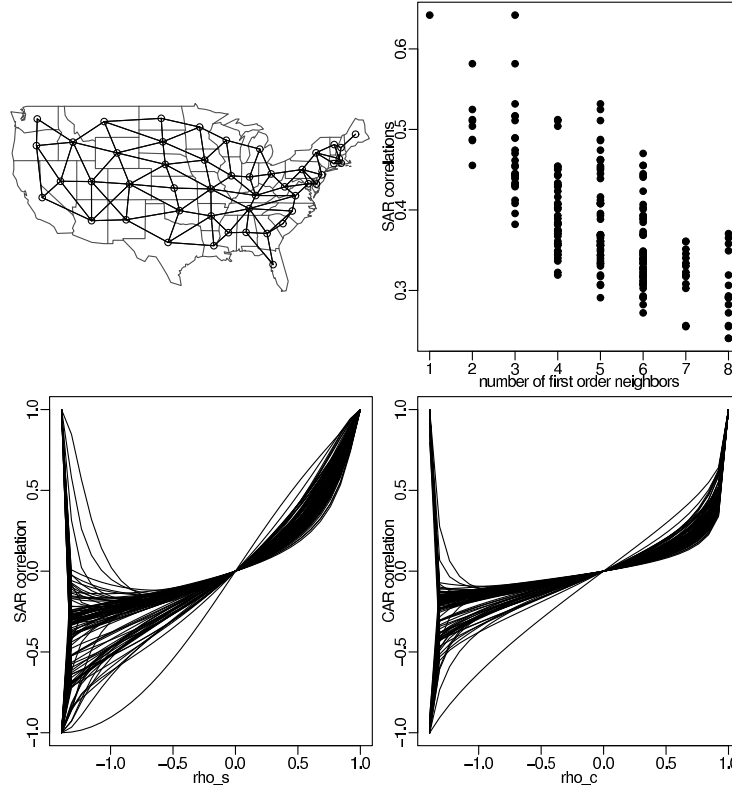


Fig. 1. The graph of USA states by neighborhood, SAR correlations implied by number o neighbors if $\rho_s = 0.6$ and the correlations implied by SAR and CAR models for all possible ρ_s and ρ_c values

137 Most of the puzzling results appear in these plots. We can see that lines cross
 138 each other as ρ varies, irrespective of the model adopted. This means that, if
 139 we increase the spatial correlations between all pairs of areas by increasing ρ ,
 140 states which are less correlated than others can become more correlated after
 141 varying ρ . For example, when $\rho_c = 0.49$, the correlation between Alabama
 142 and Florida is 0.1993 while the correlation between Alabama and Georgia

143 is 0.1561. However, when $\rho_c = 0.97$, the correlation between Alabama and
 144 Florida is 0.6311, smaller than the correlation between Alabama and Georgia,
 145 which is equal to 0.6490. This seems odd as it means that the effect of changing
 146 ρ is not uniquely defined.

147 Consider the behavior of $\text{Cor}(i, j)$ when ρ approaches its lower bound -1.392.
 148 the pairwise correlations approach either -1 or $+1$. The latter limit value is
 149 counter-intuitive: some pairs tend to be perfectly positively correlated when
 150 we expect they to be the opposite of their neighboring values according to the
 151 SAR or CAR models.

152 Some results are reassuring. The correlations increase monotonically with ρ
 153 when the spatial dependence parameter is positive. However, the range of
 154 the correlations depends on the value of ρ . For instance, when $\rho_s = 0.1$,
 155 correlations between neighboring states vary between 0.026 and 0.115, while
 156 this variation lies between 0.241 and 0.642 when $\rho_s = 0.6$.

157 **3 Some preliminary definitions and results**

158 To explain the puzzling consequences, we use linear algebra and graph theory
 159 results.

160 *3.1 Random graphs and the matrix W*

161 The \mathbf{W} matrix can be seen as the transition matrix of a Markov chain defined
 162 on a graph. Assume that n nodes or vertices, represented by the areas A_i , are
 163 connected by undirected edges such that there is an edge between areas i and

164 j if $w_{ij} \neq 0$. Define a discrete-time and finite Markov chain with transition
 165 matrix given by \mathbf{W} . That is, if a particle is in one vertex i at time t , it moves
 166 to a different vertex in the next moment choosing among the neighbors of A_i
 167 with equal probability. These type of Markov models are called random walks
 168 on graphs (Brémaud, 1999, page 214), or random graph, for short. \mathbf{W}^k is the
 169 transition matrix for the chain movements in k steps.

170 The random walk on the neighborhood graph converges to a unique stationary
 171 distribution if the Markov chain defined by \mathbf{W} is ergodic and aperiodic. For
 172 this, the graph must be connected, i.e., from each node there exists a path of
 173 edges connecting successive nodes until any other arbitrarily chosen node is
 174 reached. If \mathbf{W} is the normalized adjacency matrix of an undirected graph \mathbf{G} ,
 175 then the stationary distribution of the Markov chain defined by \mathbf{W} is given
 176 by $\boldsymbol{\pi} = (\pi_1, \dots, \pi_n)$ where $\pi_i = d_i/D$, where d_i is the number of neighboring
 177 areas of i and $D = \sum_i d_i$ (see Brémaud, 1999, page 214).

178 This implies that the power \mathbf{W}^k converge to a matrix composed by identi-
 179 cal rows, all of them equal to the stationary distribution vector $\boldsymbol{\pi}$. That is,
 180 $\mathbf{W}_{ij}^k \rightarrow d_j/D$, as $k \rightarrow \infty$. The convergence to this stationary distribution is
 181 geometric, with relative speed proportional to the second-largest eigenvalue
 182 modulus. This result is known as the Perron-Fröbenius theorem (Brémaud,
 183 1999, page 157). and it is important for our development. It can be shown
 184 that the eigenvalue of \mathbf{W} with the largest modulus has multiplicity 1 and it
 185 is $\lambda = 1$. Let $\lambda_2, \dots, \lambda_n$ be the other eigenvalues of \mathbf{W} ordered in a such a
 186 way that

$$187 \quad \lambda_1 = 1 \geq |\lambda_2| > \dots \geq |\lambda_n|.$$

188 Let m_2 be the multiplicity of λ_2 and $\mathbf{1} = (1, \dots, 1)^t$. Then, the Perron-
 189 Fröbenius theorem proves that

$$190 \quad \mathbf{W}^k = \mathbf{1} \, \pi^t + O(k^{m_2-1} |\lambda_2|^k),$$

191 where k is a positive constant. In particular, if $|\lambda_2| > |\lambda_3|$ then $m_2 = 1$ and
 192 the convergence speed decays exponentially with the second largest eigenvalue
 193 modulus $|\lambda_2|$.

194 3.2 A matrix identity

195 There is a matrix identity which is fundamental to understanding the behavior
 196 of the correlations implied by the models and described in Section 2. If \mathbf{M}
 197 is a square matrix such that each entry of the matrix \mathbf{M}^k goes to zero as k
 198 increases, then the inverse $(\mathbf{I} - \mathbf{M})^{-1}$ exists and is given by

$$199 \quad (\mathbf{I} - \mathbf{M})^{-1} = \mathbf{I} + \mathbf{M} + \mathbf{M}^2 + \mathbf{M}^3 + \dots \quad (6)$$

200 (see Iosifescu, 1980, page 45). Take $\mathbf{M} = \rho \mathbf{W}$ where $|\rho| < 1$. Since $0 \leq \mathbf{W}_{ij}^k \leq$
 201 1 for all i, j and for all integer k , we can write

$$202 \quad (\mathbf{I} - \rho \mathbf{W})^{-1} = \mathbf{I} + \rho \mathbf{W} + \rho^2 \mathbf{W}^2 + \rho^3 \mathbf{W}^3 + \dots \quad (7)$$

203 3.3 The powers of the \mathbf{W} matrix

204 If $[\mathbf{W}^k]_{ij} > 0$, then the probability of going from i to j in k steps in the
 205 random graph is positive. This means that there exists at least one sequence
 206 of k edges connecting nodes such that the initial and final nodes are i and j ,

207 respectively. Let us call such a path of a k -th order path between areas i and
 208 j . In fact, the value of $[\mathbf{W}^k]_{ij}$ is a weighted sum of all the k -th order paths
 209 between i and j . For example, $[\mathbf{W}^2]_{ij}$ is given by

$$210 \quad [\mathbf{W}^2]_{ij} = \sum_{k=1}^n W_{ik} W_{kj} = \sum_{k=1}^n \frac{a_{ik}}{d_i} \frac{a_{kj}}{d_k} = \frac{1}{d_i} \sum_{k=1}^n \frac{a_{ik} a_{kj}}{d_k} . \quad (8)$$

211 The binary product $a_{ik} a_{kj}$ is equal to 1 only if k connects both i and j .
 212 Therefore, $[\mathbf{W}^2]_{ij}$ is proportional to a weighted sum of all second-order paths
 213 $i \rightarrow k \rightarrow j$. Each path contributes a fraction inversely proportional to the
 214 number d_k of neighbors the intervening area k has. The more connected k
 215 is, the smaller the contribution of the path $i \rightarrow k \rightarrow j$ to $[\mathbf{W}^2]_{ij}$. Note that
 216 $[\mathbf{W}^2]_{ii} > 0$ because there is at least one path of the type $i \rightarrow k \rightarrow i$ since each
 217 area has at least one neighbor.

218 Similarly, $[\mathbf{W}^3]_{ij}$ is given by

$$219 \quad [\mathbf{W}^3]_{ij} = \sum_{l=1}^n [\mathbf{W}^2]_{il} w_{lj} = \frac{1}{d_i} \sum_{l=1}^n \sum_{k=1}^n \frac{a_{ik} a_{kl} a_{lj}}{d_k d_l} . \quad (9)$$

220 Each path $i \rightarrow k \rightarrow l \rightarrow j$ is inversely weighted by how dense is the neigh-
 221 borhood graph at k and l . Note that paths such as $i \rightarrow j \rightarrow i \rightarrow j$ are also
 222 counted.

223 4 Revisiting the puzzling results

224 Putting together the results of Section 3, for $|\rho| < 1$, we can write

$$225 \quad [(\mathbf{I} - \rho \mathbf{W})^{-1}]_{ij} = [\mathbf{I}]_{ij} + \rho [\mathbf{W}]_{ij} + \rho^2 [\mathbf{W}^2]_{ij} + \rho^3 [\mathbf{W}^3]_{ij} + \dots \quad (10)$$

231 and for some value k , we can write

232

$$[(\mathbf{I} - \rho \mathbf{W})^{-1}]_{ij} \approx [\mathbf{I}]_{ij} + \rho[\mathbf{W}]_{ij} + \dots + \rho^{k-1}[\mathbf{W}^{k-1}]_{ij} + \frac{d_j \rho^k}{D(1 - \rho)} \quad (11)$$

$$\approx [\mathbf{I}]_{ij} + \rho[\mathbf{W}]_{ij} + \dots + \rho^{k-1}[\mathbf{W}^{k-1}]_{ij} \quad (12)$$

233 With these facts, the results are less puzzling and easier to understand. Ba-
 234 sically, when we naively try to understand the covariance structure focusing
 235 only on the first-order neighborhood structure, we are doomed from the start.
 236 For instance, if the third degree approximation in (12) suffices, we have the
 237 CAR model covariance between areas i and j , $i \neq j$, given approximately by

$$238 \quad \frac{\kappa^2}{d_j} \left(\frac{\rho a_{ij}}{d_i} + \frac{\rho^2}{d_i} \sum_{k=1}^n \frac{a_{ik} a_{kj}}{d_k} + \frac{\rho^3}{d_i} \sum_{l=1}^n \sum_{k=1}^n \frac{a_{ik} a_{kl} a_{lj}}{d_l d_k} \right)$$

239 Ignoring the neighborhood structure geographically more distant than the first
 240 order will produce a crude approximation to the true correlation coefficient.
 241 Giving due consideration to the longer paths from i to j , though with ever
 242 decreasing weight, we find the results described by Wall (2004) to be much
 243 less puzzling, as we discuss next.

244 4.1 The CAR model with $\rho_c > 0$

245 First, let us consider the CAR model and $\rho_c > 0$. Then, (10) shows that the
 246 correlation must increase monotonically with ρ_c , since all the coefficients in
 247 that series expansion are nonnegative. This is one of the empirical results from
 248 Wall (2004). Although it is what one expects intuitively, now we understand
 249 the underlying reason for this monotone increase of $\text{Cor}(i, j)$.

250 However, correlations of different pairs can increase at different rates. This is

Table 1

Values of the entries of \mathbf{W}^k , $\rho^k \mathbf{W}^k$, and the cumulative sum $\sum_{j=0}^k \rho^j \mathbf{W}^j$ for the pairs of neighboring states (Alabama, Florida) and (Alabama, Georgia). We consider the values $\rho = 0.97$ and $\rho = 0.49$.

k	1	2	3	4	5	10	30	50	100
Alabama and Florida, $\rho_c = 0.97$									
\mathbf{W}^k	0.2500	0.0500	0.0984	0.0498	0.0588	0.0317	0.0127	0.0100	0.0094
$\rho^k \mathbf{W}^k$	0.2425	0.0470	0.0898	0.0441	0.0505	0.0233	0.0051	0.0022	0.0004
$CumSum$	0.2425	0.2895	0.3794	0.4235	0.4740	0.6246	0.8345	0.8997	0.9526
Alabama and Georgia, $\rho_c = 0.97$									
\mathbf{W}^k	0.2500	0.1562	0.1516	0.1333	0.1179	0.0754	0.0312	0.0249	0.0234
$\rho^k \mathbf{W}^k$	0.2425	0.1470	0.1383	0.1180	0.1012	0.0556	0.0125	0.0054	0.0011
$CumSum$	0.2425	0.3895	0.5278	0.6458	0.7470	1.1026	1.6092	1.7711	1.9030
Alabama and Florida, $\rho_c = 0.49$									
$\rho^k \mathbf{W}^k$	0.1225	0.0120	0.0116	0.0029	0.0017	0.0000	0.0000	0.0000	0.0000
$CumSum$	0.1225	0.1345	0.1461	0.1490	0.1506	0.1517	0.1517	0.1517	0.1517
Alabama and Georgia, $\rho_c = 0.49$									
$\rho^k \mathbf{W}^k$	0.1225	0.0375	0.0178	0.0077	0.0033	0.0001	0.0000	0.0000	0.0000
$CumSum$	0.1225	0.1600	0.1778	0.1855	0.1889	0.1915	0.1915	0.1915	0.1915

251 because the series expansion coefficients in (10) are pair-specific. In fact, the

252 derivative of $[(\mathbf{I} - \rho\mathbf{W})^{-1}]_{ij}$ is equal to

$$253 \quad \frac{\partial}{\partial \rho} [(\mathbf{I} - \rho\mathbf{W})^{-1}]_{ij} = [\mathbf{W}]_{ij} + 2\rho[\mathbf{W}^2]_{ij} + 3\rho^2 [\mathbf{W}^3]_{ij} + \dots \quad (13)$$

254 This implies that, for $\rho \in (0, 1)$, we have an increasing derivative with ρ . If ρ
 255 is not too close to 1, the rate of increase of this derivative depends mostly on
 256 the second-order neighborhood $[\mathbf{W}^2]_{ij}$.

257 Different pairs can exchange their relative positions as $\rho_c > 0$ increases and
 258 it is clear now why and when this happens. The derivative on (13) depends
 259 of the specific pair i, j under consideration. For example, assuming that the
 260 second degree polynomial approximation in (12) is good enough, then

$$261 \quad \frac{\partial}{\partial \rho} [(\mathbf{I} - \rho\mathbf{W})^{-1}]_{ij} \approx [\mathbf{W}]_{ij} + 2\rho[\mathbf{W}^2]_{ij} \quad (14)$$

262 Therefore, the larger ρ_c , the greater the positive contribution of the second-
 263 order neighborhoods. Hence, when ρ_c is small, a pair (i, j) can have a small
 264 correlation that may increases faster than the correlation in other areas simply
 265 because its second order coefficient $[\mathbf{W}^2]_{ij}$ is relatively large.

266 This is the explanation for the apparently strange behavior of the switching
 267 ranks between the correlations of Alabama and Florida and Alabama and
 268 Georgia. We use Table 1 to illustrate our arguments focusing on the CAR
 269 model with $\rho_c = 0.97$ and $\rho_c = 0.49$. For Alabama and Florida,

$$270 \quad [(\mathbf{I} - \rho\mathbf{W})^{-1}]_{\text{Al, Fl}} \approx 0.25\rho + 0.05\rho^2 + 0.10\rho^3 + 0.05\rho^4 + \dots$$

271 while, for Alabama and Georgia, we have

$$272 \quad [(\mathbf{I} - \rho\mathbf{W})^{-1}]_{\text{Al, Ge}} \approx 0.25\rho + 0.16\rho^2 + 0.15\rho^3 + 0.13\rho^4 + \dots$$

273 The coefficients of this expansion has a slower decline for the more fully con-
 274 nected pair (Alabama, Georgia) than for the pair (Alabama, Florida). When
 275 $\rho = 0.49$, this difference is not relevant because the diminishing ρ^k quickly
 276 shrinks the term $\rho^k[\mathbf{W}^k]_{ij}$ towards zero for both pairs. The consequence is
 277 that the first few terms, with small k , dominate the series. Considering only
 278 the first order approximation with k , we are within 64% and 81% of their
 279 limiting values, equal to 0.1915 for the pair (Alabama, Georgia), and equal
 280 to 0.1517 for the pair (Alabama, Florida), respectively. Using a third degree
 281 approximation with $k = 3$, we get very close to these limits, within 93% and
 282 96%, respectively.

283 This picture changes substantially when $\rho = 0.97$. Now, even relatively large
 284 k -th order neighborhoods contribute a fair amount to the series sum. As a
 285 consequence, the convergence of $[(\mathbf{I} - \rho\mathbf{W})^{-1}]$ is slow. With $k = 1$, we are
 286 within only 13% and 25% from their limiting values, equal to 1.9030 for the
 287 pair (Alabama, Georgia), and equal to 0.9526 for the pair (Alabama, Florida),
 288 respectively. Increasing to $k = 10$ we are still away from the limiting values,
 289 58% from (Alabama, Georgia), and 66% from (Alabama, Florida). This means
 290 that more geographically distant neighborhood structures, reflected in the k
 291 steps paths from i to j in the \mathbf{W}^k entries, have a non-negligible impact on
 292 the series' limits. Since these paths are different for the two pairs of areas, the
 293 end result is that an initial ordering of correlations when $\rho = 0.49$ is switched
 294 as ρ increases to 0.97.

295 Let us turn our attention to the relationship between variances $\text{Var}(y_i)$ and the
 296 number d_i of first order neighbors. Wall (2004) noticed that there is a typical
 297 negative relationship between these two quantities but that there is also vari-
 298 ation of $\text{Var}(y_i)$ among areas with equal d_i . We use again the approximation

299 in (12) to clarify this in the case of the CAR model.

300 Suppose that the \mathbf{W}^k converge fast enough such that

301

$$\begin{aligned}
\text{Var}(y_i) &= \frac{\sigma_c^2}{d_i} [(\mathbf{I} - \rho \mathbf{W})^{-1}]_{ii} \\
&\approx \frac{\sigma_c^2}{d_i} \left(1 + \rho[\mathbf{W}]_{ii} + \rho^2[\mathbf{W}^2]_{ii} + \frac{d_i \rho^3}{D(1 - \rho)} \right) \\
&= \frac{\sigma_c^2}{d_i} \left(1 + \rho^2[\mathbf{W}^2]_{ii} \right) + \frac{\sigma_c^2 \rho^3}{D(1 - \rho)} \\
&\approx \frac{\sigma_c^2}{d_i} \left(1 + \frac{\rho^2}{d_i} \sum_k \frac{a_{ik} a_{ki}}{d_k} \right)
\end{aligned}$$

302 where, in the last approximation, we ignored the last term and used (12). The
303 declining value of $\text{Var}(y_i)$ with d_i is obvious but we also need to recognize the
304 effect of the second (and higher) neighborhood order. The sum $\sum_k (a_{ik} a_{ki})/d_k$
305 depends on its number of terms. That is, it depends on the number d_i of first
306 order neighbors $k \sim i$. It also depends on the connectedness degree of these
307 neighbors through their d_k values.

308 To illustrate with an extreme case, suppose that area i has a single neighbor,
309 area k . Then

$$310 \quad \text{Var}(y_i) \approx \sigma_c \left(1 + \frac{\rho^2}{d_k} \right)$$

311 Two areas in this same single-neighbor situation have different variances if
312 their single neighbors have different number of neighbors. The more connected
313 is the single neighbor k , the smaller the variance of i .

314 4.2 The CAR model with $\rho_c < 0$

315 Concerning the negative pairwise correlations, again the spatial dependence
 316 parameter ρ_c and the higher order neighboring areas are crucial to understand
 317 their behavior. For $-1 < \rho_c < 0$, the terms in the series (10) alternate signs and
 318 this explains the counter intuitive behavior of some pairs of areas. If ρ is close
 319 to its lower bound -1 , the decay ρ^k is slow and more distant neighborhood
 320 patterns impact on the correlation value with alternating signs. The first term
 321 $\rho[\mathbf{W}]_{i,j}$ in the covariance expansion (10) is obviously negative. However, since
 322 $[\mathbf{W}^k]_{i,j}$ is not a monotone decreasing function of k , it is possible that the
 323 sum of the first two brings the covariance closer to zero or even positive. This
 324 happens if an increase in $[\mathbf{W}^2]_{i,j}$ with respect to $[\mathbf{W}]_{i,j}$ more than compensates
 325 the decrease from $|\rho|$ to ρ^2 . This argument is valid with higher order of k .

326 As an example, consider Vermont and Massachusetts. When $\rho_c = -0.99999$,
 327 the correlation between these two areas is equal to -0.1051 . The convergence
 328 of $[(\mathbf{I} - \rho\mathbf{W})^{-1}]_{ij}$ for this pair is very slow. Table 2 shows the values \mathbf{W}^k ,
 329 $\rho^k\mathbf{W}^k$, and the cumulative sum $\sum_{j=0}^k \rho^j\mathbf{W}^j$ for Vermont and Massachusetts.
 330 We can see that the cumulative sum alternates widely. The difference between
 331 $k = 100$ and $k = 101$ for the cumulative sum is in the second decimal place,
 332 a substantial value for such a large order k .

333 All pairs of neighboring areas have negative correlation in the CAR model
 334 when $-1 < \rho_c < 0$. However, in the SAR model with $\rho_s = -0.9999$, Vermont
 335 and Massachusetts has correlation equal to 0.0293 . We discuss the SAR model
 336 in more detail in section 4.3 but it is appropriate to advance some of its results
 337 here. Similarly to the CAR model, using the power expansion of $[(\mathbf{I} - \rho\mathbf{W})^{-1}]$

Table 2

Values of the entries of \mathbf{W}^k , $\rho^k \mathbf{W}^k$, and the cumulative sum $\sum_{j=0}^k \rho^j \mathbf{W}^j$ for the pairs (Vermont, Massachusetts). We consider $\rho = -0.99999$.

k	1	2	3	4	5	10	100	101
W^k	0.3333	0.1778	0.1948	0.2061	0.1729	0.1590	0.0315	0.0313
$\rho^k W^k$	-0.3300	0.1778	-0.1948	0.2061	-0.1729	0.1590	0.0315	-0.0313
$CumSum$	-0.3300	-0.1556	-0.3504	-0.1442	-0.3172	-0.1151	-0.1671	-0.1984

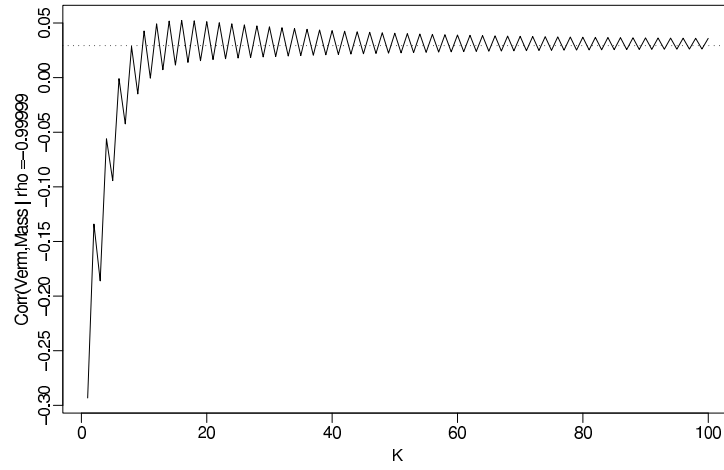


Fig. 2. Successively approximating the correlation between Vermont and Massachusetts as we increase the number of terms in the finite sums of (15). We use $\rho_s = -0.9999$.

for the SAR covariance in (5), we can express $\text{Cor}(i, j)$ as a power series in ρ_s .
 Figure 2 shows the approximation as successively larger finite sums are used
 to approximate the eventually positive correlation. Considering only the first
 neighborhood orders, the approximation is negative.

The behavior for $\rho \leq -1$ is less simple to explain with our tools. The series
 expansion (10) is no longer valid and our interpretations can not be put into
 use. When an extremely negative spatial parameter is used in the US states

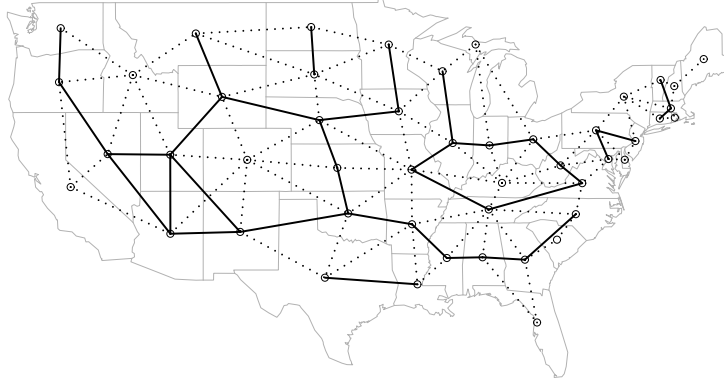


Fig. 3. Edges of US states neighborhood graph drawn according to the pairwise correlation when ρ_c approaches its lower bound -1.3923 . Solid line: positive correlations, $+1$; dashed line: negative correlations, -1 .

graph, the pairwise correlations approach either to -1 or to $+1$. In Figure 3 we draw the edges according to the limiting behavior of the pairwise correlation as ρ_c approaches its lower bound $-1.3923 = \min_i \{\lambda_i\}^{-1}$. A virtually identical figure is obtained for the SAR model. Solid lines are used for those pairs in which the correlation approach -1 while the dashed lines represent the pairs with limiting correlation approaching $+1$. It is not clear what the pattern means but we present a conjecture. We suggest the hypothesis that areas located at the center of star shaped local neighborhoods have their connecting edges mostly negative. See, for example, Idaho, Colorado, and South Dakota. The edges composing the outer rings of these star-shaped local neighborhoods have positive correlations.

To consider an intuitive explanation for this conjecture, imagine that we are going to assign the value $+1$ to approximately one half of the areas and -1 to the remaining areas. In this way we keep the global mean close to zero. Let B be the number of neighboring edges connecting areas with different values.

360 If we want to maximize B , it seems that assigning $+1$ to the center of star
 361 shaped areas and -1 to the areas in the outer rings may be near optimal. We
 362 are investigating the truth of our conjecture at the moment.

363 4.3 The SAR model

364 The arguments for the SAR model are very similar to those presented for the
 365 CAR model but the formulas are more convoluted. Using the power series
 366 expansion (10) in the SAR covariance (5), we can write

$$\begin{aligned}\Sigma_s &= (I - \rho \mathbf{W})^{-1} \Lambda((I - \rho \mathbf{W})^{-1})' \\ &= (I + \rho \mathbf{W} + \rho^2 \mathbf{W}^2 + \rho^3 \mathbf{W}^3 + \dots) \Lambda(I + \rho \mathbf{W} + \rho^2 \mathbf{W}^2 + \rho^3 \mathbf{W}^3 + \dots)' \\ &= \sum_{n=0}^{\infty} \left[\rho^n \sum_{k=0}^n \mathbf{W}^k \Lambda(\mathbf{W}^{n-k})' \right]\end{aligned}$$

367 which has elements given by

$$368 \quad (\Sigma_s)_{ij} = \frac{\sigma_s}{d_j} \sum_{n=0}^{\infty} \left[\rho^n \sum_{k=0}^n (\mathbf{W}^k)_{ij} (\mathbf{W}^{n-k})_{ji} \right] \quad (15)$$

369 If the third degree approximation for $(I - \rho \mathbf{W})^{-1}$ suffices then

$$370 \quad (\Sigma_s)_{ij} = \sum_{k=1}^n (I - \rho \mathbf{W} + \rho^2 \mathbf{W} + \rho^3 \mathbf{W}^3)_{ik} \frac{\sigma^2}{d_k} (I - \rho \mathbf{W} + \rho^2 \mathbf{W} + \rho^3 \mathbf{W}^3)_{jk} \quad (16)$$

371 where the element $(I - \rho \mathbf{W} + \rho^2 \mathbf{W} + \rho^3 \mathbf{W}^3)_{ik}$ is equal to

$$372 \quad I_{\{i=k\}} - \rho \frac{a_{ik}}{d_i} + \frac{\rho^2}{d_i} \sum_{p=1}^n \frac{a_{ip} a_{pk}}{d_p} + \frac{\rho^3}{d_i} \sum_{p=1}^n \sum_{q=1}^n \frac{a_{ip} a_{pq} a_{qk}}{d_p d_q} \quad (17)$$

373 The main difference between SAR and CAR is that a third degree approx-
 374 imation for $(I - \rho \mathbf{W})^{-1}$ imply in up to a sixth degree polynomial in ρ_s for
 375 each entry of the covariance matrix, the coefficients involving elements of \mathbf{W} .
 376 Therefore, we get the same type of polynomial approximation as in the CAR

377 model and our qualitative conclusions follow unchanged for the SAR model.
 378 Incidentally, note that this higher approximating polynomial degree in the
 379 SAR model as compared to the CAR model explains why, in Figure 1, the
 380 first order neighbor correlations increase at a slower rate as a function of pos-
 381 itive ρ_c in the CAR model than for positive ρ_s in the SAR model. For a given
 382 approximating polynomial in ρ for $(I - \rho \mathbf{W})^{-1}$, the implied SAR correlation
 383 polynomial has more positive terms than the corresponding CAR polynomial,
 384 as can be seen in (), for example.

385 4.4 *The role of $|\lambda_2|$*

386 The second largest eigenvalue modulus $|\lambda_2|$ is in the interval $[0, 1)$ and it is
 387 responsible for the speed at which $[\mathbf{W}^k]_{ij}$ converges to its limiting value d_j .
 388 That is, the smaller $|\lambda_2|$, the smaller the degree k required in the approxima-
 389 tion (12). Regular graphs are those with d_i constant. For a highly irregular
 390 neighborhood graph it is difficult to obtain exact results analytically. However,
 391 on regular graphs, these results are available and they highlight the interplay
 392 between the neighborhood structure and the approximation speed (See Chung,
 393 1997, Chapter 1). Basically, the more connected the graph is, the larger the
 394 value of $|\lambda_2|$. Hence, $|\lambda_2|$ is a measure of overall connectedness of a graph.

395 In order to illustrate these points, we computed $|\lambda_2|$ for some regular graphs.
 396 Consider a ring graph with nodes $\{(u, u + 1) : 1 \leq u < n^2\} \cup \{(1, n^2)\}$.
 397 Then, $|\lambda_2| = \cos(2\pi/n^2) \approx 1$ if n is large (Chung, 1997, page 6). This de-
 398 creases substantially when we pass to a grid graph with n^2 vertices sym-
 399 metrically wrapped into a torus. In this case, each vertex has four neigh-
 400 boring vertices and $|\lambda_2| = (1 + \cos(2\pi/n))/2$, the midpoint between 1 and

401 $\cos(2\pi/n) < \cos(2\pi/n^2)$ for $n \geq 2$. Finally, consider the most dense graph
 402 possible with n^2 vertices, the complete graph in which every area is a neigh-
 403 bor of every other area. Then, $|\lambda_2| = 1/(n^2 - 1) \approx 0$, if n^2 is large.

404 Admittedly, these graphs are highly artificial and do not represent the typical
 405 maps found in practice. To have a better idea of the effect of the average
 406 density of connections on $|\lambda_2|$, and hence on the speed of the convergence
 407 $[\mathbf{W}^k]_{ij} \rightarrow d_j/D$, we successively pruned a real map while keeping the entire
 408 graph connected. The objective is to show how the value of $|\lambda_2|$ tends towards
 409 1 as we prune the graph.

410 The usual US states map is not the best choice for this demonstration. The
 411 reason is that $|\lambda_2| = 0.9714$ for this graph, a large initial value. This large
 412 value indicates that there are parts of the map (such as the NE region) that
 413 are hard to reach in a random walk, implying in long paths or a nearly discon-
 414 nected graph. Even more regularly connected graphs have large eigenvalues.
 415 Therefore, in addition to pruning the usual adjacency neighborhood graph, we
 416 also added edges between second-order neighbors. That is, we increased the
 417 density of connections in the graph by adding edges between areas that are
 418 separated from each other by at most a third area.

419 We randomly selected an edge to be deleted while this was possible until only
 420 $n - 1$ edges remained (that is, until we reached a spanning tree). We also
 421 randomly created edges between second-order neighbors. To keep the balance
 422 on the two directions, we added edges until we reached the same number
 423 needed to generate the most pruned graph. We repeated this procedure one
 424 hundred times independently.

425 Figure 4 shows the graph of the second largest eigenvalue modulus $|\lambda_2(j)|$

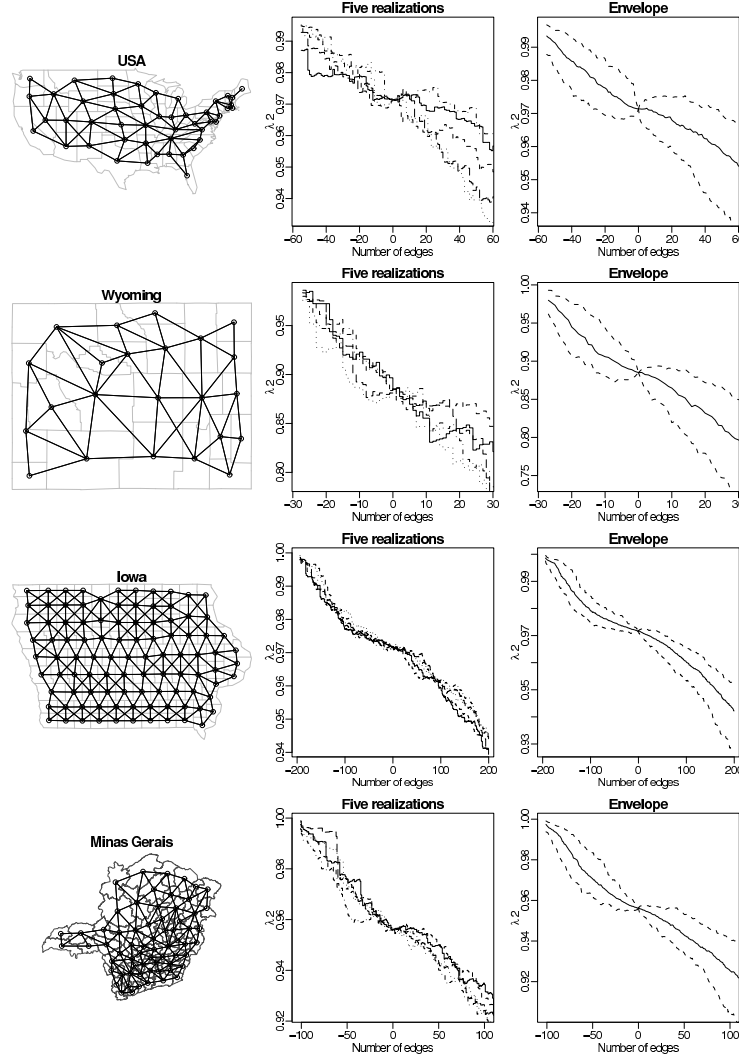


Fig. 4. Sucessively adding or pruning the adjacency neighborhood graph of four graphs. The geographical regions are the US states map, the the counties of Wyoming and Iowa, and the municipalities of Minas Gerais, a Brazilian state. The second column of plots shows five realizations of the of the addition-pruning process in each graph. The third column of plots shows 95% confidence envelopes based on the simulations in dashed lines, as well as the mean $|\lambda_2(j)|$ value in solid line.

where j is either the number of deleted edges from the original map (if $j < 0$)
or the number of added edges (if $j > 0$). We used four geographical regions,
shown in the first column of plots: the US states map, the counties of Wyoming
and Iowa, and the municipalities of Minas Gerais, a Brazilian state with the

430 same extension as France. Their $|\lambda_2(0)|$ values are 0.9714, 0.8850, 0.9717, and
431 0.9561, respectively. The second column of plots shows five realizations of
432 the addition-pruning process in each graph. Each line is the value of $|\lambda_2(j)|$
433 as j varies. The third column of plots shows in dashed lines 95% confidence
434 envelopes based on the 100 simulations, as well as the mean $|\lambda_2(j)|$ value as a
435 solid line.

436 Specific paths within the confidence envelope are not necessarily monotone.
437 That is, the deletion (or addition) of a specific edge can decrease (or increase)
438 the eigenvalue of the resulting \mathbf{W} matrix. However, the average behavior is
439 that the denser the connections, the smaller the eigenvalue and hence, faster
440 the convergence. In terms of the puzzling results discussed in Wall(2004), this
441 means that the denser the graph, the less likely the change of ranks between
442 different pairs of areas.

443 5 Conclusions

444 We found a systematic structure to the SAR and CAR covariance model asso-
445 ciated with the spatial structure of the data. This structure is not determined
446 only by the immediate neighborhood of each area. Rather, in a very precise
447 way, we show that the spatial covariance depends on the spatial connections
448 of all neighborhood orders. How strong is the impact of more distant neigh-
449 boring areas is determined by the second largest eigenvalue modulus of the
450 neighborhood matrix \mathbf{W} and the value of the spatial dependence parameter
451 ρ .

452 **References**

- 453 [6] Besag, J. and Kooperberg, C. (1995) On conditional and intrinsic au-
454 toregressions. *Biometrika*, 82, 733–746.
- 455 [6] Brémaud P. (2001) *Markov Chains*. Springer-Verlag, New York.
- 456 [6] Chung, F. R. K. (1997) *Spectral Graph Theory*. CBMS Regional Confer-
457 ence Series in Mathematics, volume 92. American Mathematical Society:
458 Providence.
- 459 [6] Haining, R. (1990) *Spatial Data Analysis in the Social and Environmental*
460 *Sciences*. Cambridge University Press, Cambridge.
- 461 [6] Iosifescu, M. (1980) *Finite Markov Processes and Their Applications*.
462 John Wiley and Sons: New York.
- 463 [6] Wall, M. (2004) A close look at the spatial structure implied by the
464 CAR and SAR models. *Journal of Statistical Planning and Inference*,
465 121, 311–324.